BIG BANG NUCLEOSYNTHESIS

PREDICTIONS - SUMMARY

- T(t) from rel. particles
  - PHOTONS
  - NEUTRINOS
- N'SYN IN FEW MINUTES
  - ^2H
  - A = 5, 8 BOTTLENECKS
- ^1H, ^2H, ^3He, ^4He, ^7Li predicted for $\eta = n_B/n_\gamma$ from CMB power spectrum

TRACE OF BARYONS $\left\{ \begin{array}{l} = 6 \times 10^{-10} \\ \Omega_b h^2 = 0.022 \end{array} \right.$

UNCERTAINTIES: $\tau(n)$, $\langle \sigma v \rangle_{ij}$ [N_ν]

V. SMALL!

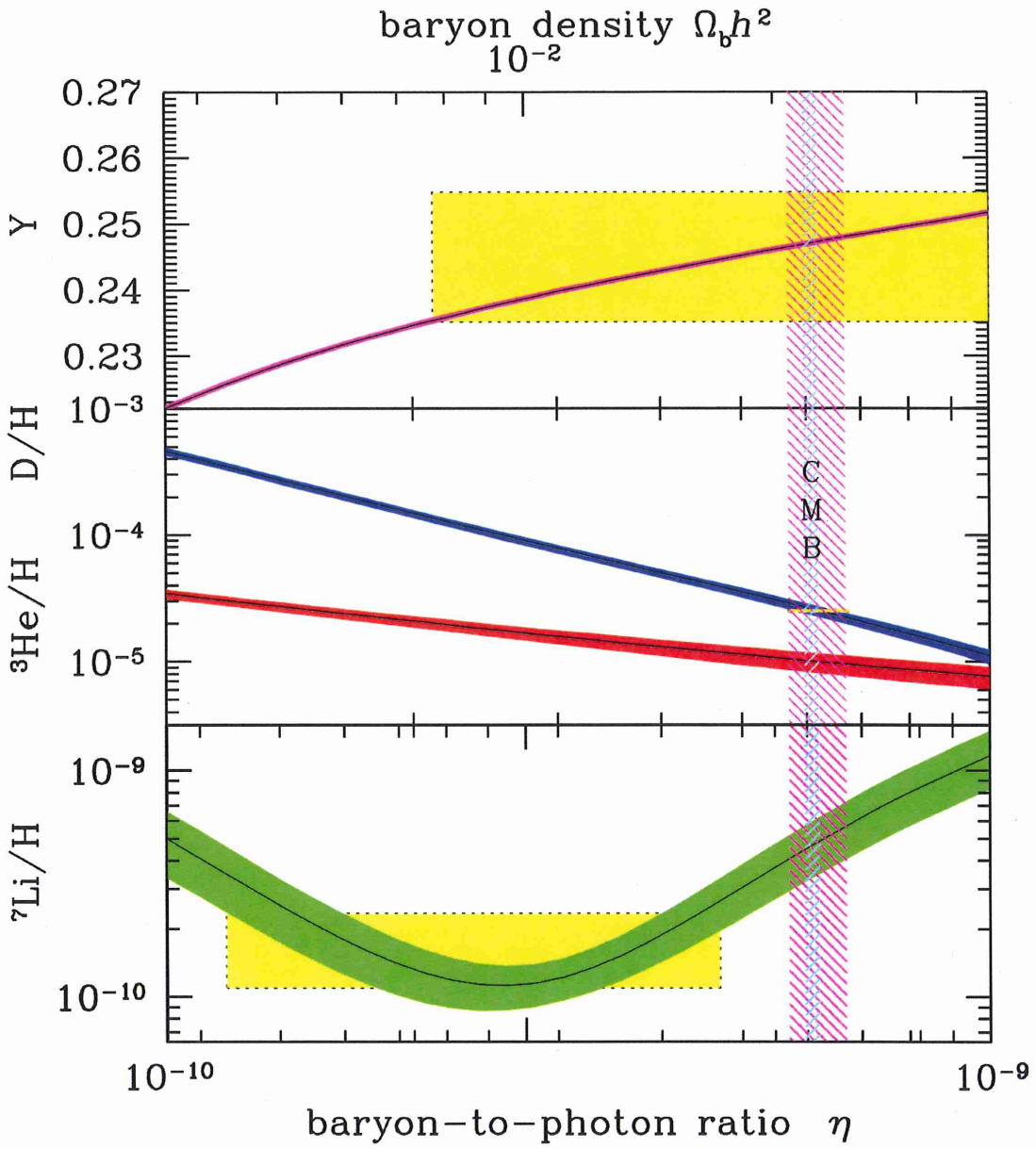

Figure 23.1: The abundances of ^{4}He, D, ^{3}He, and ^{7}Li as predicted by the standard model of Big-Bang nucleosynthesis — the bands show the 95% CL range [5]. Boxes indicate the observed light element abundances. The narrow vertical band indicates the CMB measure of the cosmic baryon density, while the wider band indicates the BBN concordance range (both at 95% CL).

$Y_p^{BBN} = 0.253 \pm 0.025$

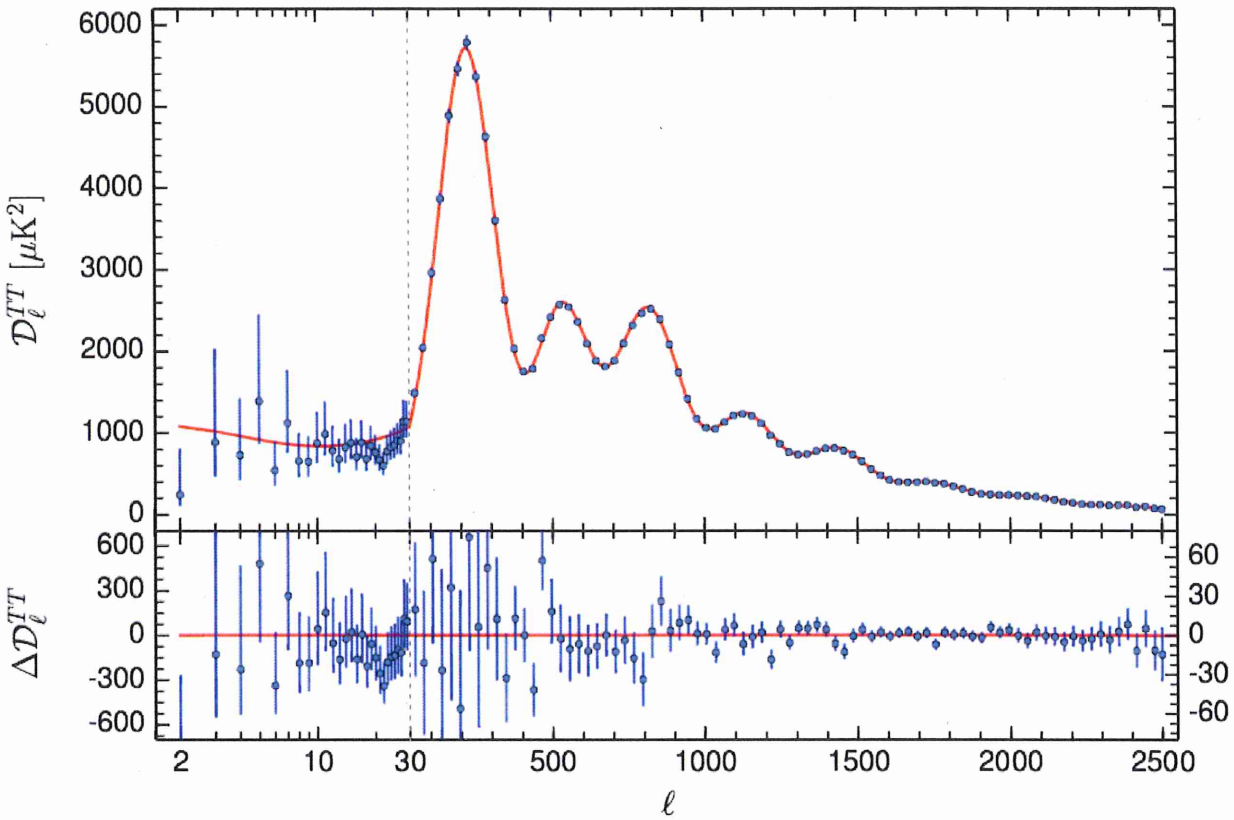

Fig. 1. The *Planck* 2015 temperature power spectrum. At multipoles $\ell \approx 30$ we show the maximum likelihood frequency averaged temperature spectrum computed from the Plik cross-half-mission likelihood with foreground and other nuisance parameters determined from the MCMC analysis of the base ΛCDM cosmology. In the multipole range $2 \approx \ell \approx 29$, we plot the power spectrum estimates from the Commander component-separation algorithm computed over 94% of the sky. The best-fit base ΛCDM theoretical spectrum fitted to the *Planck* TT+lowP likelihood is plotted in the upper panel. Residuals with respect to this model are shown in the lower panel. The error bars show $\pm 1\,\ell$ uncertainties.

sults to the likelihood methodology by developing several independent analysis pipelines. Some of these are described in Planck Collaboration XI (2015). The most highly developed of these are the CamSpec and revised Plik pipelines. For the 2015 *Planck* papers, the Plik pipeline was chosen as the baseline. Column 6 of Table 1 lists the cosmological parameters for base ΛCDM determined from the Plik cross-half-mission likelihood, together with the lowP likelihood, applied to the 2015 full-mission data. The sky coverage used in this likelihood is identical to that used for the CamSpec 2015F(CHM) likelihood. However, the two likelihoods differ in the modelling of instrumental noise, Galactic dust, treatment of relative calibrations and multipole limits applied to each spectrum.

As summarized in column 8 of Table 1, the Plik and CamSpec parameters agree to within $0.2\,\ell$, except for n_s, which differs by nearly $0.5\,\ell$. The difference in n_s is perhaps not surprising, since this parameter is sensitive to small differences in the foreground modelling. Differences in n_s between Plik and CamSpec are systematic and persist throughout the grid of extended ΛCDM models discussed in Sect. 6. We emphasise that the CamSpec and Plik likelihoods have been written independently, though they are based on the same theoretical framework. None of the conclusions in this paper (including those based on the full "TT,TE,EE" likelihoods) would differ in any substantive way had we chosen to use the CamSpec likelihood in place of Plik. The overall shifts of parameters between the Plik 2015 likelihood and the published 2013 nominal mission parameters are summarized in column 7 of Table 1. These shifts are within $0.71\,\ell$ except for the parameters ℓ and $A_s e^{-2\ell}$ which are sensitive to the low multipole polarization likelihood and absolute calibration.

In summary, the *Planck* 2013 cosmological parameters were pulled slightly towards lower H_0 and n_s by the $\ell \approx 1800$ 4-K line systematic in the 217 × 217 cross-spectrum, but the net effect of this systematic is relatively small, leading to shifts of $0.5\,\ell$ or less in cosmological parameters. Changes to the low level data processing, beams, sky coverage, etc. and likelihood code also produce shifts of typically $0.5\,\ell$ or less. The combined effect of these changes is to introduce parameter shifts relative to PCP13 of less than $0.71\,\ell$, with the exception of ℓ and $A_s e^{-2\ell}$. *The main scientific conclusions of PCP13 are therefore consistent with the 2015 Planck analysis.*

Parameters for the base ΛCDM cosmology derived from full-mission DetSet, cross-year, or cross-half-mission spectra are in extremely good agreement, demonstrating that residual (i.e. uncorrected) cotemporal systematics are at low levels. This is

$Y_p = 0.326 \pm 0.075$

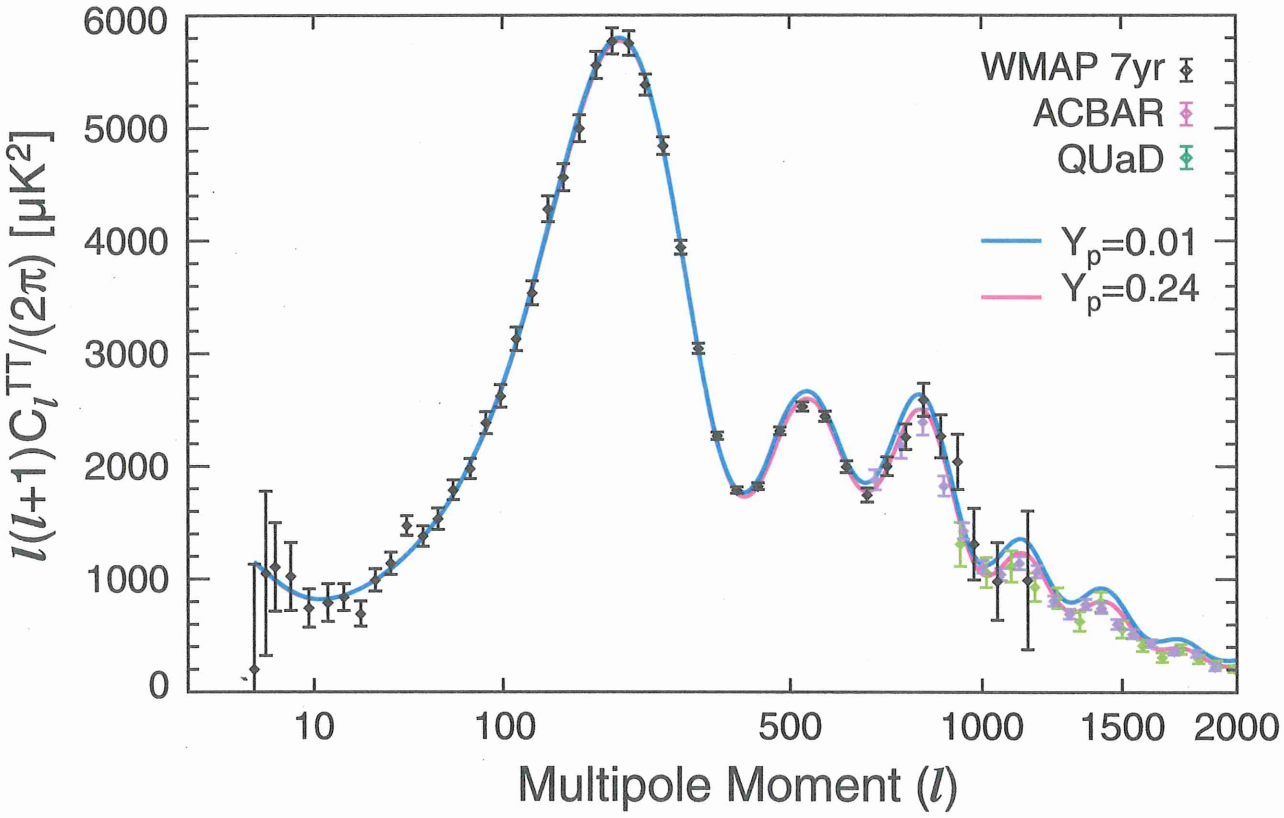

FIG. 10.— Primordial helium abundance and the temperature power spectrum. The data points are the same as those in Figure 7. The lower (pink) solid line (which is the same as the solid line in Figure 7) shows the power spectrum with the nominal helium abundance, $Y_p = 0.24$, while the upper (blue) solid line shows that with a tiny helium abundance, $Y_p = 0.01$. The larger the helium abundance is, the smaller the number density of electrons during recombination becomes, which enhances the Silk damping of the power spectrum on small angular scales, $l \gtrsim 500$.

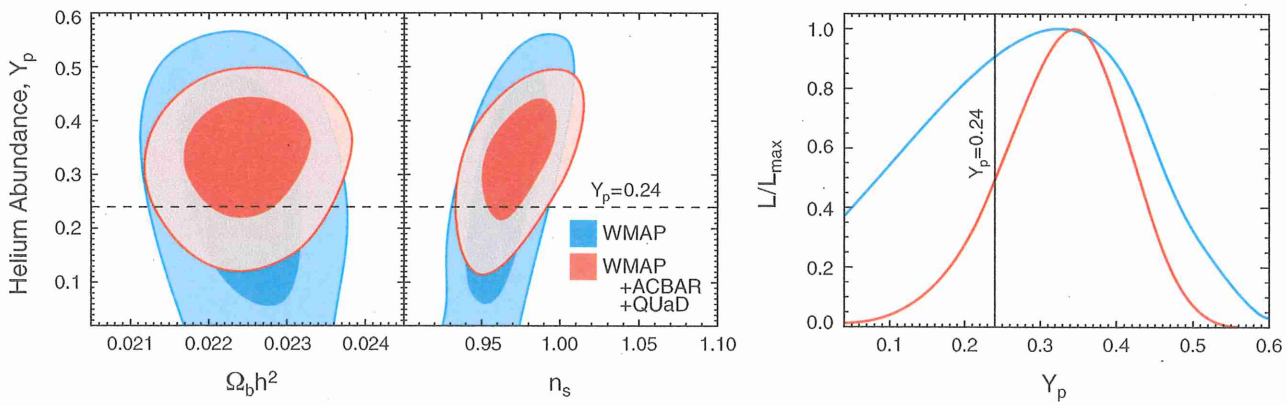

FIG. 11.— Constraint on the primordial helium abundance, Y_p. (Left) Joint two-dimensional marginalized distribution (68% and 95% CL), showing that Y_p and $\Omega_b h^2$ are essentially uncorrelated. (Middle) A slight correlation exists between Y_p and n_s: an enhanced Silk damping produced by a larger Y_p can be partially canceled by a larger n_s. (Right) One-dimensional marginalized distribution of Y_p from *WMAP*-only and *WMAP*+ACBAR+QUaD. The 68% interval from *WMAP*+ACBAR+QUaD, $Y_p = 0.326 \pm 0.075$ is consistent with the nominal value, 0.24, which is shown by the vertical line.

enhanced Silk damping produced by a larger Y_p can be partially canceled by a larger n_s (Trotta & Hansen 2004).

We find a 95% CL upper limit of $Y_p < 0.51$ from the *WMAP* data alone. When we add the ACBAR and QUaD data, *we find a significant detection of the effect of primordial helium by more than* 3σ (see the right panel of Figure 11),

$$Y_p = 0.326 \pm 0.075 \text{ (68\% CL)}.$$

The 95% CL limit is $0.16 < Y_p < 0.46$. The 99% CL lower limit is $Y_p > 0.11$. This value is broadly consistent with the helium abundances estimated from observations of low-metallicity extragalactic ionized (HII) regions, $Y_p \simeq 0.24 - 0.25$ (Gruenwald et al. 2002; Izotov & Thuan 2004; Olive & Skillman 2004; Fukugita & Kawasaki 2006; Peimbert et al. 2007). See Steigman (2007) for a review.

We can improve this limit by imposing an *upper limit* on Y_p from these astrophysical measurements. As the helium is created by nuclear fusion in stars, the he-

OBSERVATIONAL TESTS OF BBN

- DIRECT via CMB POWER SPECTRUM
  - HeIH via high l

    $Y_p = 0.253 \pm 0.025$

    from PLANCK
- INFERRED from VERY METAL-POOR SYSTEMS
  - X/H vs products of n/synthesis and extrapolate to $n/s \to 0$

DO INFERRED ABUNDANCES OF

- ^2H, ^3He, ^4He, and ^7Li

  ≡ PREDICTED ABUNDANCES FOR η(PLANCK)?

- OTHER NUCLIDES - ^6Li, ^9Be, ^{10}B, ^{11}B, ^{12}C, ...

  ≡ ZERO

→ IF NO, IS SOLUTION TO BE SOUGHT IN

- OBSERVATIONS
- PREDICTIONS
  - STD. INGREDIENTS
  - NON-STD. BIG BANG.

$^4He/H$

HISTORY - a few points

- HOYLE & TAYLER (1964)
- STELLAR EVOLUTION (1960s +)
  - He color-mag diagram
    ≃ He/H of young massive stars yet ~ Fe/H ↓100 times
  - Hot halo stars: some have
    He/H ~ 1/1000 NOT 1/10 (normal)
    CHEMICALLY PECULIAR!

... BLUE COMPACT GALAXIES
I Zw 18, II Zw 40 are O-poor
but He/H ≃ normal
(SEARLE & SARGENT 1972)

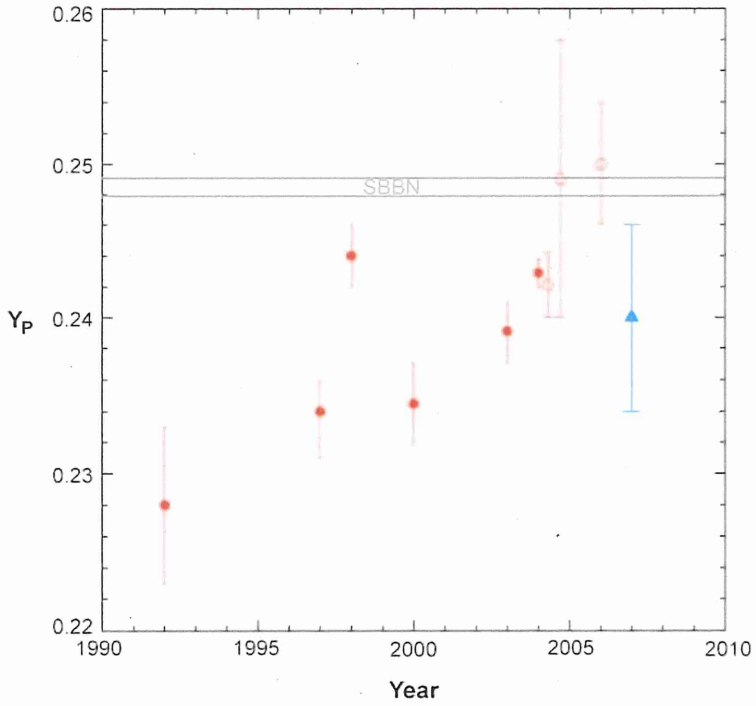

Steigman G. 2007.
Annu. Rev. Nucl. Part. Sci. 57:463–91

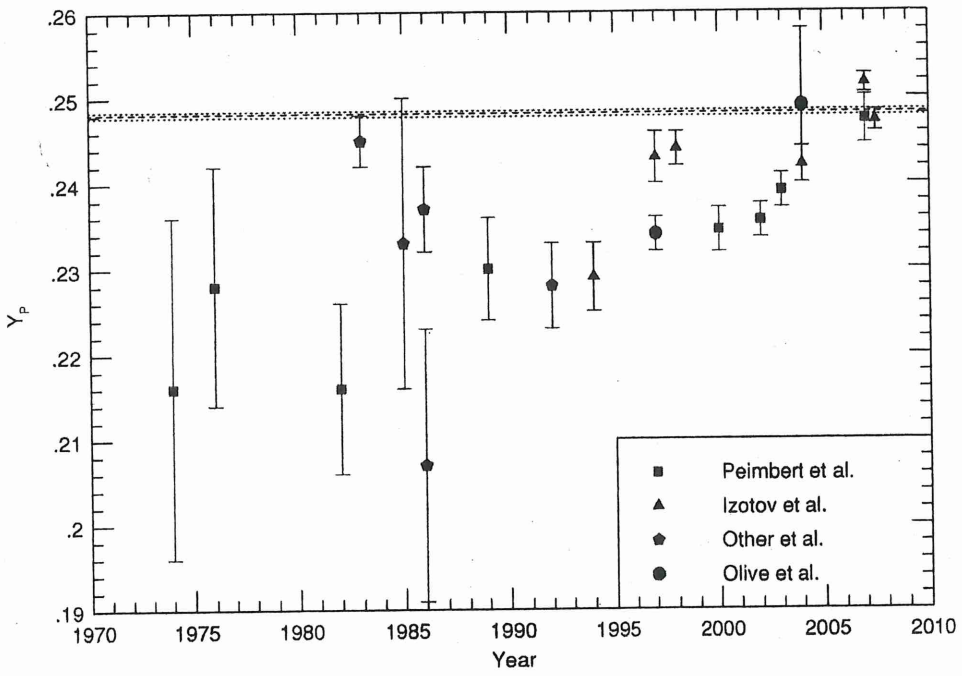

Figure 1. Historical evolution of the observational determinations of the primordial helium abundance. The solid horizontal line with dashes shows the value inferred from WMAP observations and BBN calculations.

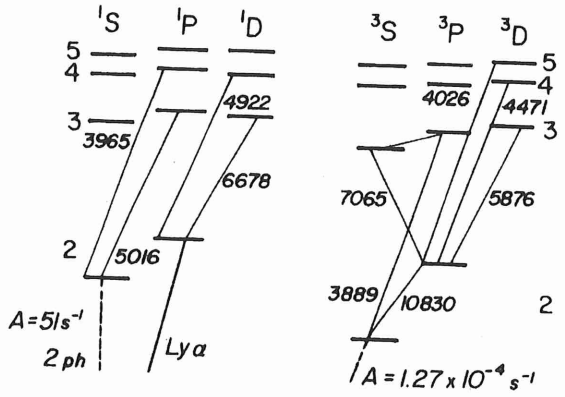

Fig. 4.9. Term scheme for He I, showing some of the transitions of interest.

In recent years, intensive efforts have been made to improve the determination of the pre-Galactic helium abundance (generally assumed to be the same as Y_P) and $\Delta Y/\Delta Z$ from observations of extragalactic H II regions. Advantages of this method are:

- The theory of recombination for hydrogen and helium seems to be well understood, at least to 1 or 2 per cent, and the line intensities are not very sensitive to temperature or density; in particular, there is no exponential factor.
- Low abundances (extending down to [O/H] $\simeq -1.5$ in the case of I Zw 18) ensure that little extrapolation to $Z = 0$ is needed.
- One can assure oneself that neutral helium is negligible by assessing that the effective temperatures of the ionizing stars are high enough (say, above 40 000 K). One way to do this is to compare the degrees of ionization of oxygen (O II/O III) and sulphur (S II/S III), which have widely differing ionization potentials, with predictions from numerical photo-ionization models.

There are also difficulties:

- Experimental problems: signal:noise, detector linearity (Hα/λ 6678 is typically about 100), calibration, reddening.
- Underlying absorption lines in the stellar continuum.
- Line absorption in the intervening interstellar gas, or Earth's atmosphere.
- Fluorescence and collisional excitation, arising primarily from the metastability of the 2^3S level (see Fig. 4.9), in which consequently a high population accumulates which can cause additional emission from lines such as λ 4471, λ 5876 by either collisional excitation or radiative transfer effects following absorption of higher lines in the $2^3\mathrm{S} - n^3\mathrm{P}$ series. The singlet line λ 6678 can also be enhanced by collisional excitation from 2^3S. The collisional effects can be calculated from the known electron temperature and density, and are quite small at

typical electron densities of the order of 100 cm^{-3} except in the case of λ 7065. The latter line, once collisional effects are allowed for, can also be used to gauge the influence of radiative transfer effects, which are normally found to be small for extragalactic H II regions. Collisional excitation can also slightly affect the hydrogen lines, especially Hα, when the electron temperature is high, i.e. at the lowest metallicities (Davidson & Kinman 1985).

- While the triplet levels exist only from $n = 2$ upwards, the singlets have an analogue to the hydrogen Lyman-α line and consequently, like hydrogen, have Cases A and B (or intermediate). The assumption of Case B, which is usually made, could be slightly inaccurate if Ly-α were to either partially escape or be absorbed by small amounts of dust in the nebula. However, the above-mentioned lines are not very sensitive to Case A or B, while λ 5016, which is very sensitive because of the strong transition from its upper state 3^1P to the ground state 1^1S, is found to be in agreement with Case B whenever it is measured.
- Temperature gradients and local temperature fluctuations usually parameterized by t^2 (Peimbert 1967) lead to a systematic bias when the electron temperature determined conventionally from [O III] λ 4363/λ 5007 is substituted into the expressions for effective recombination coefficients of hydrogen and helium.
- $\Delta Y/\Delta Z$ or $\Delta Y/\Delta$(O/H) may vary, either systematically as a function of Z or randomly, e.g. if some H II regions are self-polluted with helium and other elements (e.g. N) ejected in winds from massive embedded stars. There is some evidence that this actually happens in a very few cases, such as the nucleus of NGC 5253, where the continuum shows a strong, broad feature at the He^+ wavelength λ 4686, due to Wolf–Rayet stars.

TODAY

- MEASURE $^4He/H$ via EMISSION LINES IN EXTRAGALACTIC REGIONS AND PLOT $^4He/H$ vs O/H (or N/H) AND EXTRAPOLATE TO $O/H = 0$ TO GET Y

- DIFFICULT TO GET ERRORS - eg. SYSTEMATIC - UNDER CONTROL
  - $HeI\,H$ varies with time!
  - See Pagel's summary

- LATEST ATTEMPTS
  - IZOTOV et al. (2014) incl. 10830 Å
    $Y_p = 0.2551 \pm 0.0022$
  - AVER et al. (2015) reanalysis of above
    $Y_p = 0.2449 \pm 0.0040$

D/H

- BIG BANG = ONLY SOURCE OF D
  - STARS ASTRATE D

    EPSTEIN, LATTIMER & SCHRAMM (1976)

- DETECTIONS OF D BEYOND EARTH BEGAN IN 1970s
  - SOLAR SYSTEM CH_3D, HD
  - SOLAR WIND from $^3He/^4He$
  - ISM D I Lyman lines in UV
  - DEUTERATED MOLECULES IN ISM / MOL. CLOUDS FRACTIONATION!
  - H II REGIONS Dα next to Hα

↓

- CAN BE DIFFICULT TO GET D/H
- IS DIFFICULT (GCE) TO CORRECT D/H FOR ASTRATION OVER AGE OF GALAXY

Abstract. The detection and first identification of the deuterium Balmer emission lines, Dα and Dβ, in the core of the Orion Nebula is reported. These lines are very narrow, have identical 11 km s^{-1} velocity shifts with respect to Hα and Hβ, are probably excited by UV continuum fluorescence from the Lyman (D I) lines and arise from the interface between the H II region and the molecular cloud.

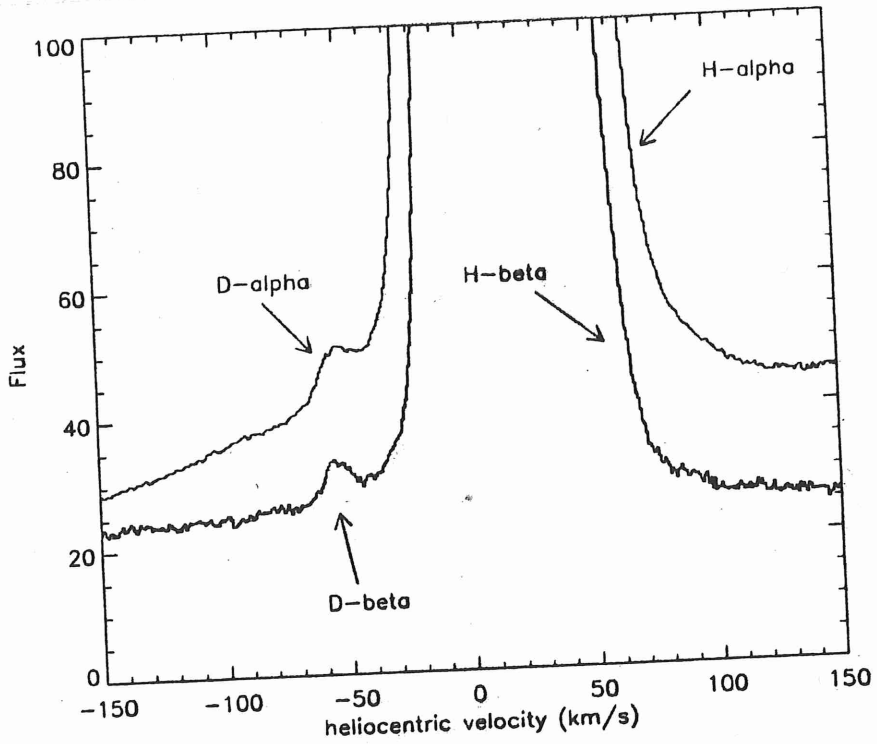

Fig. 1. Vicinity of Hα and Hβ in Orion, showing Dα and Dβ in emission. The x-axis is in km s^{-1} relative to the rest wavelength of either Hα or Hβ. The vertical scale corresponds to peak fluxes 7250 and 2500 for Hα and Hβ respectively. Then $I(\mathrm{H}\alpha)/I(\mathrm{H}\beta) = 2.91$ and $I(\mathrm{D}\alpha)/I(\mathrm{D}\beta) \simeq 1.10$.

Hébrard et al. 2000, A&A, 354, L79

TO THE QSOs

- ADAMS (1976) proposed Lyman line spectrum of QSOs.
  1st ATTEMPT IN 1994 WAS IN ERROR! ($DH = 2.5 \times 10^{-4}$)
- FEW QSOs ARE SUITABLE
  - COLUMN DENSITY
    $17 < \log N(HI) < 21$
  - LOW METALLICITY
  - LOW TURBULENCE ($b_{50}.\Delta v = 81.6$ km/s)
  - SIMPLE CLOUD STRUCTURE
    = NO HI INTERLOPERS

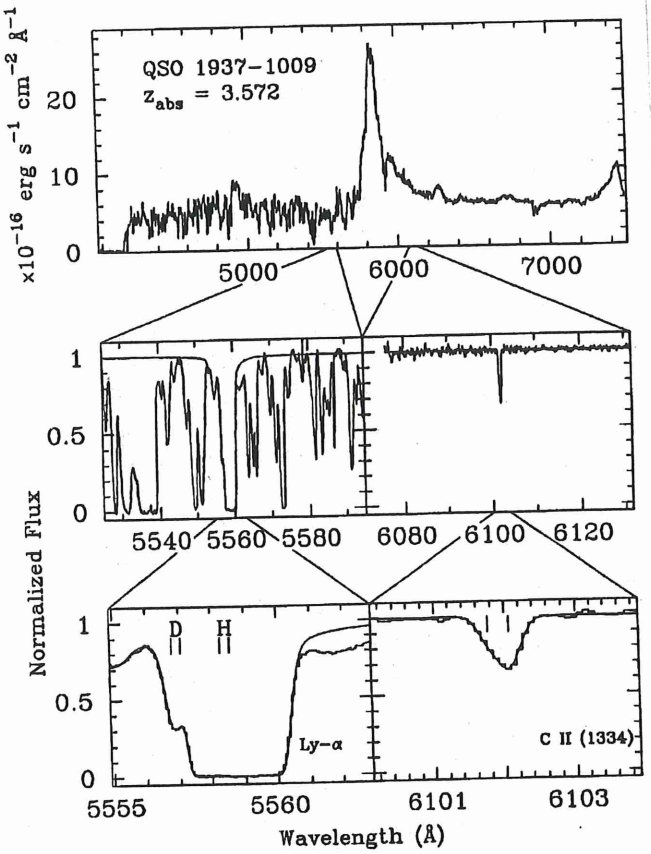

FIG. 2. Spectra of quasar Q1937-1009. Top panel: Low-resolution spectrum taken with the Shane three-meter telescope at Lick Observatory. The prominent feature at 5850 Å is Ly-α emission from the quasar. The depression shortward of 4200 Å is Lyman-continuum absorption from the deuterium cloud at $z = 3.572$. The hundreds of absorption lines (Ly-α forest) are due to individual hydrogen clouds along the line of sight. Middle and bottom panels: Keck HiRes spectra of Q1937-1009. Middle panel shows the deuterium cloud lying within the resolved Ly-α forest (left) and the singly ionized carbon line due to the deuterium cloud lying in isolation. Bottom panel shows the model fit to the Ly-α lines of the two deuterium and hydrogen components (resolved by their metal lines). Figure courtesy of S. Burles.

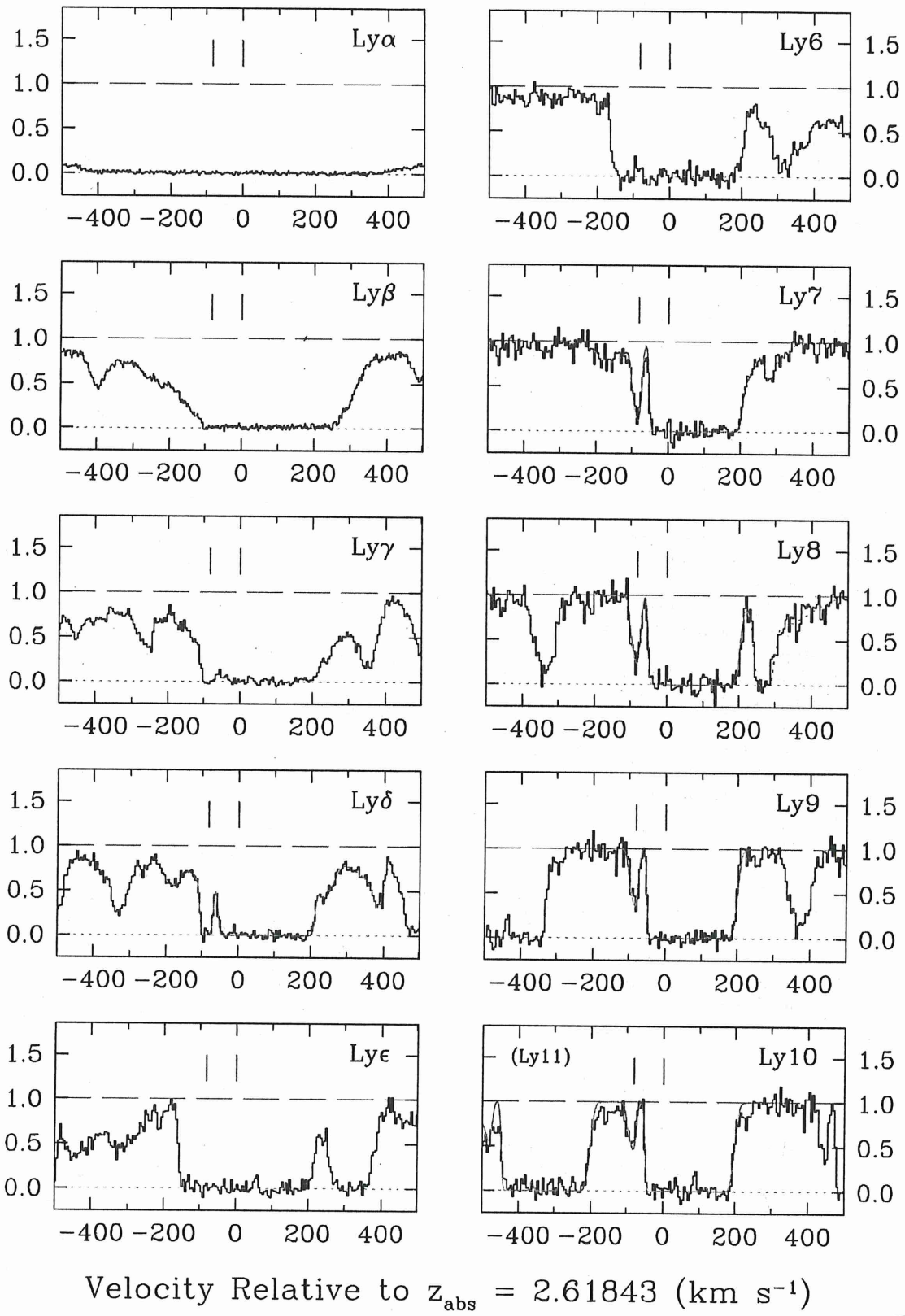

Figure 1. Observed profiles (black histograms) and fitted Voigt profiles (continuous red lines) of absorption lines in the Lyman series of the $z_{abs} = 2.61843$ DLA in Q0913+072. The y-axes of the plots show relative intensity. The two vertical tick marks in each panel indicate the expected locations of the main absorption component of the DLA in, respectively, H I (at $v = 0\,\mathrm{km\ s^{-1}}$ in the plots) and D I (at $v = -81.6\,\mathrm{km\ s^{-1}}$). A second absorption component, centred at $v = -12.4\,\mathrm{km\ s^{-1}}$, is resolved in the metal lines associated with this DLA, but the two components are blended in the intrinsically broader H I and D I absorption. Additional H I absorption is seen at positive velocities relative to the DLA, but its column density is ~100 times lower than that of the DLA and therefore does not contribute to the observed D I absorption lines (see text).

RECENT RESULTS FOR D/H

- COOKE et al. (2014, ApJ, 781:31)

$$\langle D/H \rangle = (2.53 \pm 0.04) \times 10^{-5}$$

≡ BBN prediction &
independent of N(HI) and OH

$^3He/H$

- SOLAR SYSTEM
  - TRAPPED GAS IN METEORITES

    $^3He/^4He = 1.54 \pm 0.30 \ 10^{-5}$

    IN JUPITER

    $= 1.66 \pm 0.05 \ 10^{-5}$
  - STARS
    - NOT DETECTED IN NORMAL STARS ?
    - CHEMICALLY PECULIAR STARS

      3 CEN A $^3He/^4He \sim 1$
  - ISM
    - PICKUP IONS

      $^3He/H = 2.48 \pm .6 \times 10^{-5}$

- HII REGIONS AND PLANETARY NEBULAE

  $^3He^+$ 8.7 GHz spin-flip transition

  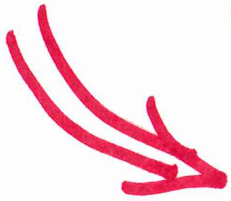

  HEROIC EFFORT

- LOW MASS STARS MAKE ^3He AND MAY ENRICH ISM WITH ^3He

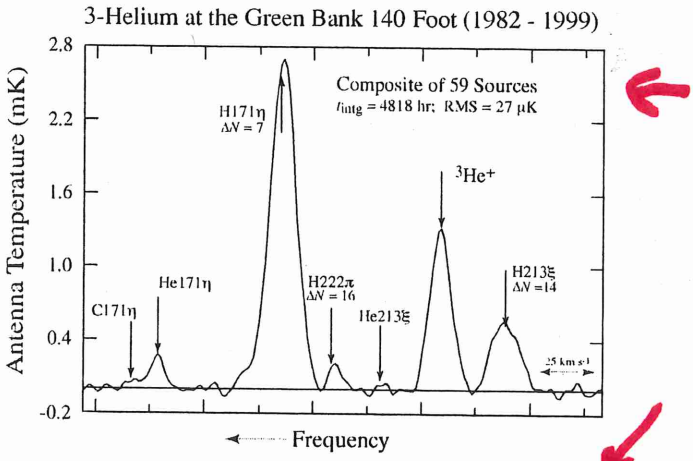

Figure 3. NRAO 140-Foot H II region composite ^{3}He spectrum. This 200 day integration is the most sensitive cm-wavelength spectrum ever taken. Besides the $^3He^+$ emission, a variety of recombination lines from H, ^{4}He, and C are seen. Many of these arise from transitions resulting from large changes in principle quantum number, e.g. H 171 η, Δ N = 7, and H 213 ξ, Δ N = 14.

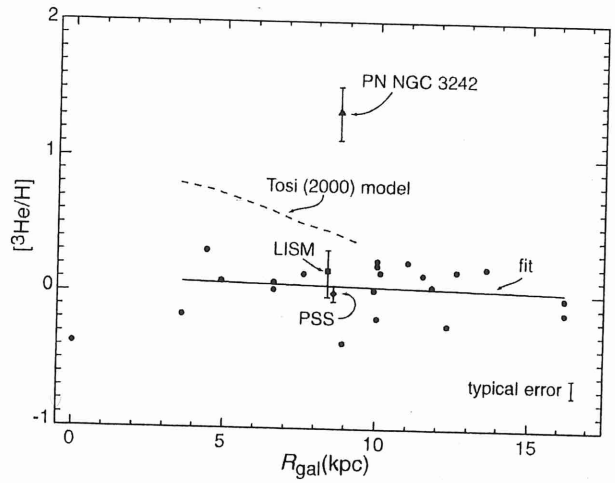

Figure 1. "The ^{3}He Problem" ^{3}He/H abundances as a function of Galactic radius. The [^{3}He/H] abundances by number for the BRB H II region sample are given with respect to the solar ratio. Shown also are the abundances for the planetary nebula NGC 3242 (triangle), the local interstellar medium (LISM—square), and protosolar material (PSS—diamond). There is no gradient in the ^{3}He/H abundance with Galactic position.

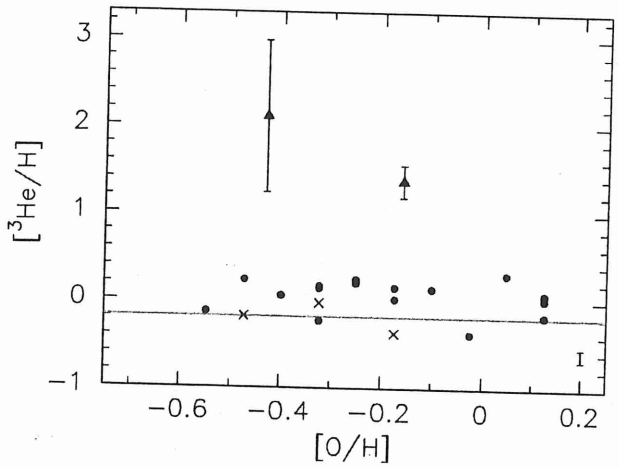

Figure 2. "The ^{3}He Plateau" [^{3}He/H] abundances as a function of source metallicity for the "simple" H II region sample. The gray line is the WMAP result. The ~ 0.15 dex typical error is shown in the right hand corner. The triangles denote abundances for the PNe J 320 (left) and NGC 3242. There is no trend in the ^{3}He/H abundance with source metallicity.